

1
2
3
4 1 **Structural analysis of different LINC complexes**
5
6 2 **reveals distinct binding modes**
7
8
9 3
10
11 4
12

13 5 **Victor E. Cruz¹, F. Esra Demircioglu¹ and Thomas U. Schwartz^{1,*}**
14

15 6 ¹Department of Biology, Massachusetts Institute of Technology, Cambridge, MA, 02139,
16
17 7 USA
18

19 8 *Corresponding author
20
21
22 9
23
24
25
26
27
28
29
30
31
32
33
34
35
36
37
38
39
40
41
42
43
44
45
46
47
48
49
50
51
52
53
54
55
56
57
58
59
60
61
62
63
64
65

1
2
3
4
5
6
7
8
9
10
11
12
13
14
15
16
17
18
19
20
21
22
23
24
25
26
27
28
29
30
31
32
33
34
35
36
37
38
39
40
41
42
43
44
45
46
47
48
49
50
51
52
53
54
55
56
57
58
59
60
61
62
63
64
65

10 **Abstract**

11 Linker of nucleoskeleton and cytoskeleton (LINC) complexes are molecular tethers that
12 span the nuclear envelope (NE) and physically connect the nucleus to the cytoskeleton.
13 They transmit mechanical force across the NE in processes such as nuclear anchorage,
14 nuclear migration, and homologous chromosome pairing during meiosis. LINC complexes
15 are composed of KASH proteins traversing the outer nuclear membrane, and SUN
16 proteins crossing the inner nuclear membrane. Humans have several SUN- and KASH-
17 containing proteins, yet what governs their proper engagement is poorly understood. To
18 investigate this question, we solved high resolution crystal structures of human SUN2 in
19 complex with the KASH-peptides of Nesprin3, Nesprin4, and KASH5. In comparison to
20 the published structures of SUN2-KASH1/2 we observe alternative binding modes for
21 these KASH peptides. While the core interactions between SUN and the C-terminal
22 residues of the KASH peptide are similar in all five complexes, the extended KASH-
23 peptide adopts at least two different conformations. The much-improved resolution allows
24 for a more detailed analysis of other elements critical for KASH interaction, including the
25 KASH-lid and the cation loop, and a possible self-locked state for unbound SUN. In
26 summary, we observe distinct differences between the examined SUN-KASH complexes.
27 These differences may have an important role in regulating the SUN-KASH network.

28
29 **Keywords**

30 SUN proteins, KASH proteins, nucleo-cytoplasmic communication, mechanotransduction,
31 nuclear envelope

32

1
2
3
4
5
6
7
8
9
10
11
12
13
14
15
16
17
18
19
20
21
22
23
24
25
26
27
28
29
30
31
32
33
34
35
36
37
38
39
40
41
42
43
44
45
46
47
48
49
50
51
52
53
54
55
56
57
58
59
60
61
62
63
64
65

33 Introduction

34 The nucleus in eukaryotic cells is physically separated from the cytoplasm by a double
35 membrane bilayer known as the nuclear envelope (NE). The outer nuclear membrane
36 (ONM) faces the cytoplasm and is contiguous with the endoplasmic reticulum (ER), while
37 the inner nuclear membrane (INM) borders the nucleoplasm. The two membranes are
38 fused at circular openings where nuclear pore complexes (NPCs) reside [1]. The lumen
39 between the INM and ONM is known as the perinuclear space (PNS), has a thickness of
40 30-50 nm and is contiguous with the lumen of the ER. Communication between the
41 nucleus and the cytoplasm across the NE is accomplished by two separate molecular
42 entities. On one hand, molecular exchange primarily occurs through the NPC [2,3]. On
43 the other hand, mechanical signaling is mediated through molecular tethers, the Linker of
44 Nucleoskeleton to Cytoskeleton (LINC) complexes [4–8].

45
46 The core of LINC complexes resides in the PNS, formed by two proteins. SUN (Sad1 and
47 UNC84) proteins traverse the INM, while KASH (Klarsicht, ANC-1 and Syne Homology)
48 proteins are tail anchored at the ONM and constitute the cytoplasmic anchor of LINC
49 complexes. SUN proteins are conserved in all eukaryotes [9,10]. They possess an N-
50 terminal domain that projects into the nucleus followed by a transmembrane helix that
51 spans the INM. The nuclear domain of SUN proteins interacts with lamins and
52 heterochromatin, anchoring SUN at the INM[11]. The perinuclear domain of SUN proteins
53 consists of an extended coiled-coil that precedes the conserved C-terminal SUN domain
54 which binds to KASH proteins[12]. To date, five SUN proteins have been identified in
55 humans. SUN1 and 2 are present in all tissues and possess partially redundant functions.
56 SUN3, 4, and 5 are expressed in testis and have a shorter coiled-coil domain than their
57 SUN1/2 counterparts[13].

1
2
3
4
5
6
7
8
9
10
11
12
13
14
15
16
17
18
19
20
21
22
23
24
25
26
27
28
29
30
31
32
33
34
35
36
37
38
39
40
41
42
43
44
45
46
47
48
49
50
51
52
53
54
55
56
57
58
59
60
61
62
63
64
65

58

59 The tail anchored KASH proteins project their ~20-30 C-terminal residues, the KASH
60 peptide, into the PNS. Their “PPPX” motif at the very C terminus of the KASH peptide is
61 most distinct, highly conserved, and required for binding to SUN proteins [14–17].
62 Currently, 6 KASH domain-containing proteins have been identified in humans. These are
63 the nesprins (nuclear envelope spectrin repeats), including Nesprin1-4, as well as KASH5
64 (CCDC155), and KASH6 (LRMP) [18–20]. Many of the known interactions of KASH
65 proteins in the cytoplasm involve cytoskeletal elements. Different Nesprins bind different
66 such elements, suggesting distinct roles for specific SUN-KASH complexes. This is
67 perhaps best illustrated by human diseases, that can result from mutations in individual
68 KASH proteins [21]. For example, KASH-less forms of Nesprin-1 and Nesprin-2 are
69 associated with neurological and muscular defects such as Emery Dreifuss muscular
70 dystrophy (EDMD) and spinocerebral ataxia[22], while mutants of Nesprin-4 are known
71 to cause deafness[23]. Clearly, a detailed molecular understanding of LINC complexes is
72 necessary to understand their distinct biological functions.

73

74 The structures of the human heterohexameric SUN2-KASH1 and SUN2-KASH2
75 complexes have been determined [15,24] and provide a general illustration of the mode
76 of interaction at the core of the LINC complex. The C-terminal ~20 kDa SUN domain of
77 SUN2 folds into a compact β sandwich, which trimerizes into a trefoil, supported by a
78 preceding three-stranded coiled-coil element. KASH1 or 2 bind at the interface between
79 adjacent SUN domains. A loop, disordered in the apo-structure, folds into a beta hairpin
80 and clamps down the KASH peptide to stabilize the interaction. This element is called the
81 ‘KASH lid’[15]. Since each SUN2 trimer binds 3 KASH peptides at once, the architecture
82 of the complex inherently increasing the interaction strength, distributing expected

1
2
3
4
5
6
7
8
9
10
11
12
13
14
15
16
17
18
19
20
21
22
23
24
25
26
27
28
29
30
31
32
33
34
35
36
37
38
39
40
41
42
43
44
45
46
47
48
49
50
51
52
53
54
55
56
57
58
59
60
61
62
63
64
65

83 mechanical force across three discrete sites within the complex. SUN2 also contains a
84 loop structure that coordinates a potassium ion ('cation loop'), which is essential for KASH
85 binding[15]. Finally, a disulfide bond can be formed between SUN2 and KASH1/2 via
86 highly conserved cysteine residues. This likely enhances LINC complex stability even
87 further[25].

88 To advance our understanding of SUN-KASH pairing, we sought to address this question
89 using structural and biochemical tools. We solved high-resolution crystal structures of
90 SUN2 in complex with KASH3, KASH4, and KASH5, which complement our previously
91 published SUN2-KASH1 and SUN2-KASH2 complexes. The new structures reveal distinct
92 binding interactions of SUN2 with different KASH peptides. In addition, we solved the
93 structure of unbound, apo-SUN2 at high resolution, suggesting a novel mechanism of
94 inactivating Sun. Taken together, this data feeds into the notion that humans have evolved
95 an elaborate LINC-complex network, with the possibility for regulation on multiple levels.

96

1
2
3
4
5
6
7
8
9
10
11
12
13
14
15
16
17
18
19
20
21
22
23
24
25
26
27
28
29
30
31
32
33
34
35
36
37
38
39
40
41
42
43
44
45
46
47
48
49
50
51
52
53
54
55
56
57
58
59
60
61
62
63
64
65

97

98 **Results**

99 **SUN2 binds to all 6 human KASH peptides**

100 To begin our study, we first examined direct binding of human SUN2 to all 6 currently
101 known KASH proteins. We co-expressed SUN2 with the predicted perinuclear KASH
102 peptides of Nesprin-1,-2,-3,-4, CCDC155 (KASH-5), or LRMP (KASH-6) in *E. coli*.
103 Throughout the text we will refer to these peptides as KASH1-6, for simplicity. KASH
104 peptides were N-terminally fused to 6 histidines, followed by a GB1 solubility tag [26], and
105 a human rhinovirus 3C cleavage site. SUN2 was expressed with a cleavable, trimerizing-
106 GCN4 (triGCN4) tag [27,28], but without an affinity tag. SUN2-KASH complexes were
107 first nickel affinity purified, thereby eliminating apo-SUN2. After proteolytically cleaving
108 GB1 from KASH and triGCN4 from SUN2, SUN2-KASH complexes were separated by
109 size exclusion chromatography, with free GB1 eluting as a separate peak. This way, we
110 were able verify stable interaction of SUN2 with all 6 KASH peptides (Fig. 1).

111

112 **Crystallographic analysis of SUN2 KASH complexes**

113 We next set out to structurally characterize SUN2 in complex with KASH3, KASH4,
114 KASH5, and KASH6 by X-ray crystallography. Using a purification strategy discussed
115 previously [27], our initial attempts yielded poorly diffracting crystals of SUN2-KASH3.
116 After analyzing the crystal packing interactions of these poorly diffracting crystals, we
117 designed SUN2 mutants in the hopes to potentially enhance crystal packing, and hence
118 produce better diffracting crystals[29]. Using this approach, we indeed obtained much
119 better diffracting crystals of SUN2 in complex with KASH3 and KASH5 after introducing 4
120 point mutations in SUN2: Q534D, T683G, M684R, and A685G. For SUN2-KASH4
121 crystals, wildtype SUN2 was used. Combined with the new tagging and purification

1
2
3
4
5
6
7
8
9
10
11
12
13
14
15
16
17
18
19
20
21
22
23
24
25
26
27
28
29
30
31
32
33
34
35
36
37
38
39
40
41
42
43
44
45
46
47
48
49
50
51
52
53
54
55
56
57
58
59
60
61
62
63
64
65

122 scheme described here we finally obtained well diffracting crystals for apo-SUN2, SUN2-
123 KASH3, SUN2-KASH4, and SUN2-KASH5. (Table 1). All structures pack into crystal
124 lattices related to those observed in previous studies, helping in solving them by molecular
125 replacement[15]. The search model used was SUN2 in complex with KASH1 (PDB code
126 4DXR), lacking both the KASH lid and KASH peptide. The general features of SUN-KASH
127 engagement are maintained in all complexes (Figure 2). SUN2 forms a trimer, in the apo-
128 and all KASH-bound forms. All KASH peptides bind at the interface between adjacent
129 SUN2 monomers despite sequence variations between KASH peptides. However, we also
130 observe a distinct difference between SUN2 bound to KASH1 or 2 as opposed to KASH3,
131 4, or 5. While KASH1 and 2 kink toward the periphery of the SUN domain, KASH3, 4, and
132 5 extend towards the neighboring KASH lid from the adjacent SUN2 monomer (Figure 2).
133 The solvent exposed surface of the KASH lid shows strong conservation that remained
134 unexplained by previous structures of SUN-KASH complexes. The binding mode we
135 observe between SUN2 and KASH3, 4, and 5, reveals that the KASH peptide extends
136 toward these residues, providing a possible explanation for the observed conservation of
137 the solvent exposed face of the KASH lid.

138

139 When KASH1, 2, 3, 4, and 5 are aligned, residues between positions 0 (the very C-terminal
140 residue of KASH) to -10 only slightly diverge (Fig. 3). The main differences are start at
141 position -11, which is either a proline or a leucine. When comparing all five KASH peptides
142 side-by-side (Fig. 3, S1), we notice that the peptides with proline in -11 form one class,
143 while the other class has a leucine in the same position. The KASH peptides do not share
144 the same binding surface with SUN2 once they exit from under the KASH lid. Both KASH1
145 and 2 take a sharp 90° turn at Pro -11 that leads the KASH peptide away from the 3-fold
146 symmetry axis and instead over a neighboring SUN monomer and towards Cys563 where

1
2
3
4
5
6
7
8
9
10
11
12
13
14
15
16
17
18
19
20
21
22
23
24
25
26
27
28
29
30
31
32
33
34
35
36
37
38
39
40
41
42
43
44
45
46
47
48
49
50
51
52
53
54
55
56
57
58
59
60
61
62
63
64
65

147 a disulfide bridge is formed. KASH3, 4, and 5 lack Pro -11, and they adopt the alternate
148 binding conformation described here.

149
150 The KASH lid adopts a similar conformation in all five complexes, but it rotates and shifts
151 slightly to accommodate side chains of different sizes present in different KASH peptides.
152 Notably, KASH sequences between position -4 and -6 of different lengths are
153 accommodated (Fig. 2,3) and are partially solvent exposed. KASH3/5 possess two
154 residues here whereas KASH1/2/4 have three. To accommodate the lacking residues at
155 positions -5 and -4, KASH3 and KASH5, respectively, form a shorter loop that still
156 maintains the correct register for the remainder of the KASH peptide. Residues preceding
157 this loop are well aligned between different KASH peptides, and so are residues after this
158 loop. The tyrosine at positions -7 clearly functions as an anchor that is critical in
159 determining the register of the KASH peptide for residues -8 to -11 and facilitates the
160 hydrogen-bonding pattern between the KASH peptide and the KASH lid. The solvent
161 exposed loop between positions -4 to -6 together with the anchoring by Tyr -7 grants
162 flexibility in the sequence and length of residues that can be accommodated between the
163 Tyr -7 and the conserved “PPPX” motif.

164

165 **The cation loop of SUN2**

166 We can resolve the electron density of the cation loop in all the structures reported here,
167 but it is especially well ordered in the high-resolution structures of the SUN2-KASH3 and
168 SUN2-KASH4 complexes (Fig. 4). The cation loop of SUN2 in complex with KASH3 is
169 identical to what is observed in the apo form of SUN2, as well as SUN2 bound to
170 KASH1/2/5. In these structures a potassium ion is coordinated at the center of the cation
171 loop by the carbonyl groups of Val 590, Gln 593, Asp 595, Asn 600, Tyr 707, and by a
172 well-ordered water molecule. Surprisingly, the cation loop of SUN2 in complex with KASH4

1
2
3
4
5
6
7
8
9
10
11
12
13
14
15
16
17
18
19
20
21
22
23
24
25
26
27
28
29
30
31
32
33
34
35
36
37
38
39
40
41
42
43
44
45
46
47
48
49
50
51
52
53
54
55
56
57
58
59
60
61
62
63
64
65

173 lacks a cation. Instead of a potassium ion this structure contains two water molecules that
174 coordinate the cation loop interactions. The first water molecule hydrogen bonds with the
175 main chain carbonyl of Val 590, Gln 593, with the main chain amide of Asp 595, and with
176 its neighboring water molecule. The second water coordinates the carbonyl of Asn 600
177 and of Tyr 707. The main chain carbonyl of Asp 595 now hydrogen bonds with the amine
178 of the Asn 600 side chain and its backbone carbonyl points outside of the cation loop. In
179 the presence of potassium, the side chain of Asp 595 pairs with the amine of the Asn 600
180 side chain, however, in the absence of potassium the side chain of Asp 595 points away
181 from the cation loop and is no longer as well ordered in our density maps.

182

183 **Internal disulfide of SUN2**

184 SUN proteins contain a pair of universally conserved cysteines (Cys 601 and Cys 705 in
185 SUN2) which form a disulfide bond that presumably stabilizes the cation loop of SUN2.
186 Additionally, this disulfide forms part of the KASH binding pocket that coordinates the
187 conserved “PPPX” motif of KASH (Fig. 5). In the context of KASH1 and KASH2, Cys 601
188 and Cys 705 of SUN2 form a disulfide. Here we observe that when SUN2 is bound to
189 KASH3, KASH4, or KASH5, these cysteines are reduced. Because of the high quality of
190 our electron density maps the redox state of Cys 601 and Cys 705 is unambiguous.

191

192 **The unbound SUN domain may form a self-blocked state**

193 The main motivation behind solving another apo-SUN2 structure was that we extended
194 the construct N-terminally back to residue 500, in the hopes of resolving a longer stretch
195 of the non-canonical trimeric coiled-coil element of SUN2. However, these additional
196 residues are not visible in the structure, suggesting that they are unstructured in the
197 context of this construct. Our new structure superimposes well with the published apo-
198 SUN structures: 0.402 Å RMSD with 4DXT[15] 0.568 Å RMSD with 3UNP[30]. All

1
2
3
4
5
6
7
8
9
10
11
12
13
14
15
16
17
18
19
20
21
22
23
24
25
26
27
28
29
30
31
32
33
34
35
36
37
38
39
40
41
42
43
44
45
46
47
48
49
50
51
52
53
54
55
56
57
58
59
60
61
62
63
64
65

199 published and trimeric SUN crystal structures pack similarly, i.e. with the KASH-lid
200 containing, ONM facing side engaging in a head-to-head contact. So far, we concluded
201 that this interaction is non-physiological, primarily on two grounds. First, this conformation
202 would sterically hinder the proper engagement of KASH peptides with the ONM, with the
203 trans-membrane segment of the KASH peptide immediately adjacent to the C-terminal
204 SUN-binding portion. Second, in the KASH-bound form the interaction surface between
205 adjacent trimers is rather small and generally does not pack well. However, in the apo-
206 form this head-to-head crystal interface has a few remarkable features (Fig. 6). In
207 comparison to the apo-form, the KASH-bound head-to-head interface is driven apart
208 substantially, while losing many of the packing contacts. The buried interface in the apo-
209 SUN2 crystal measures 2,380 Å², well in the range of stable interfaces. For KASH-bound
210 interfaces, the buried area measures below 400 Å². In addition, the KASH-lid is
211 dramatically remodeled in the apo-SUN2 form. Overlooked in previous publications, the
212 apo-conformation specifically buries the highly conserved hydrophobic residues Ile 579
213 and Leu 581 in the head-to-head interface (Fig. 6)[30]. According to PISA analysis,
214 burying these hydrophobics is the main enthalpic contribution driving the interaction.
215 Finally, the well conserved Trp 582 packs tightly against the Glu 552 - Arg 589 salt bridge
216 in the apo-form. The conservation of Ile 579, Leu 581 and Trp 582 cannot be explained
217 by the SUN-KASH interaction, in which these residues are not directly involved. On the
218 other hand, a functional, self-locked apo-state would readily explain the conservation of
219 these residues, including the Glu 552 – Arg 589 salt bridge.

220

221 **Mixed occupancy LINC complexes**

222 After confirming that the core interactions between SUN2 and KASH1-5 are similar, we
223 decided to test if a single SUN2 trimer could bind to two different KASH peptides
224 simultaneously and if there is a preference for either binding mode (Figure 7). The same

1
2
3
4
5
6
7
8
9
10
11
12
13
14
15
16
17
18
19
20
21
22
23
24
25
26
27
28
29
30
31
32
33
34
35
36
37
38
39
40
41
42
43
44
45
46
47
48
49
50
51
52
53
54
55
56
57
58
59
60
61
62
63
64
65

225 purification scheme shown in Figure 1 was used in this assay, but an additional GFP fused
226 KASH peptide was co-expressed. Since only one KASH type was affinity-tagged, pulling
227 down the other KASH type indicates a mixed LINC complex. This way, we tested if SUN2
228 could bind to KASH1 and 2 simultaneously. 6xHis-GB1-KASH2 co-purified with both,
229 SUN2 and GFP-KASH1. Similarly, 6xHis-GB1-KASH4 co-purified with SUN2 and GFP-
230 KASH3. These results show that one SUN2-trimer can bind different KASH peptides at
231 once that share the same binding mode. We were also able to purify SUN2 bound to both
232 6xHis-GB1-KASH2 and GFP-KASH3, simultaneously, showing that SUN2 can bind two
233 KASH peptides that adopt different binding modes. These experiments support the idea
234 that the individual KASH binding sites are independent of one another and that mixed
235 occupancy has to be considered as a means of regulating LINC complexes.

236

237

1
2
3
4
5
6
7
8
9
10
11
12
13
14
15
16
17
18
19
20
21
22
23
24
25
26
27
28
29
30
31
32
33
34
35
36
37
38
39
40
41
42
43
44
45
46
47
48
49
50
51
52
53
54
55
56
57
58
59
60
61
62
63
64
65

238 Discussion

239 Previous work has shown that SUN and KASH interactions occur with promiscuity, which
240 raises the question of how these SUN KASH bridges can be specifically assembled and
241 regulated. Here we show that SUN2 engages with a KASH peptide in at least two distinct
242 binding modes. We can speculate whether a proline or leucine in the -11 position of KASH
243 may be the determining factor to have the peptide engage in a kinked or liner manner,
244 respectively. The argument for such a determination lies within the difference between the
245 binding of KASH1/2 vs. KASH3. While KASH1/2 are kinked, KASH3 is straight. This is
246 remarkable, because these three peptides are very similar in sequence (Fig. 3B) and it is
247 suggestive that the proline to leucine change triggers the conformational change. To be
248 certain, though, this would need to be tested experimentally.

249 While we now have the structural evidence that SUN2, and most likely the close homolog
250 SUN1 as well, are inherently promiscuous in binding the 6 different KASH peptides, it is
251 not yet clear whether the same will be true for the testis-specific SUN proteins, SUN3, -4,
252 and -5. Those sequences are far enough diverged from SUN2 to preclude a definitive
253 analysis in the absence of structural data.

254 An outstanding question in the field remains the presumed higher-order assembly of LINC-
255 complexes into 2D clusters [7,31]. Such clusters are thought to be necessary in order for
256 LINC complexes to bear significant mechanical load, i.e. during nuclear migration [25,32].

257 One easy way to envision cluster formation is that KASH-proteins themselves homo-
258 oligomerize through their cytoplasmic elements. That way, KASH-proteins, together with
259 SUN-trimers, can form higher-order arrays [12]. In this model, one KASH-protein oligomer
260 bridges several SUN-trimers. This is particularly obvious, if the KASH-protein oligomer is
261 not a trimer itself. With our data that formally shows that a single SUN-trimer can bind
262 different KASH-peptides simultaneously, we also have to entertain that higher-order

1
2
3
4
5
6
7
8
9
10
11
12
13
14
15
16
17
18
19
20
21
22
23
24
25
26
27
28
29
30
31
32
33
34
35
36
37
38
39
40
41
42
43
44
45
46
47
48
49
50
51
52
53
54
55
56
57
58
59
60
61
62
63
64
65

263 clusters may consist of mixed SUN-KASH complexes. This is an aspect of LINC complex
264 biology that so far has been largely ignored. Another element that has not garnered a lot
265 of attention is the consequence of Nesprins having multiple spectrin repeats, which are
266 protein interaction domains. It is conceivable that molecular condensates, generated
267 through repetitive protein-protein interactions, will have an important role in the molecular
268 function of LINC complexes as well.

269 We observe subtle differences in the cation loop and the redox state of the close cysteines
270 601 and 705, depending on which of the five KASH peptides is bound. It remains to be
271 seen whether these differences are biologically meaningful. For example, does the
272 presence of potassium in the cation loop prevent KASH4 interaction, since it is the only
273 structure with water coordination in the cation site? Similarly, is it relevant that the C601-
274 C705 disulfide is reduced in the KASH-3,-4, and-5 bound structures? We do not find any
275 obvious reason, why we see these differences and whether or not they are influenced by
276 the KASH peptides, or whether they may simply be the result of different crystallization
277 conditions. We believe it will be interesting to see more SUN-KASH pairs structurally
278 characterized, at or near atomic resolution, to give a more detailed picture.

279 Finally, there is an ongoing debate about the regulation of the assembly state of Sun. In
280 order for SUN to bind KASH in a productive and meaningful manner, the cell has to ensure
281 that binding only occurs after SUN has reached the inner nuclear membrane, i.e. traveled
282 from its insertion site within the endoplasmic reticulum, past the circular opening around
283 NPCs, to its destination. If SUN binds KASH before passage to the INM, it will be sterically
284 blocked to pass the NPC, and therefore presumably be non-functional. One way to
285 envision that KASH engagement only happens after SUN reaches its destination is that
286 Sun is kept in a non-binding state before. Studies by the Feng lab suggest that SUN1/2
287 can adopt a monomeric, KASH-binding incompetent state[33]. In these structural studies
288 the perinuclear coiled-coil element engages with the SUN domain to occlude the KASH

1
2
3
4
5
6
7
8
9
10
11
12
13
14
15
16
17
18
19
20
21
22
23
24
25
26
27
28
29
30
31
32
33
34
35
36
37
38
39
40
41
42
43
44
45
46
47
48
49
50
51
52
53
54
55
56
57
58
59
60
61
62
63
64
65

289 binding site. Thus, one can envision that Sun is kept in this inactive form until it reaches
290 the INM. Once there, a yet-to-be-identified signal could switch SUN from inactive to active.
291 We hypothesize that the head-to-head self-locked apo-SUN structure we observe may
292 better reflect a KASH-binding inhibited state. First, the monomeric SUN form described in
293 [33] is dependent on a specific coiled-coil truncation being present. Whether this is
294 representative of the behavior of full-length SUN is not proven, a significant limitation to
295 the study. In contrast, for our self-locked structure, there is no principal concern why it
296 could not be physiologically relevant. In fact, since the self-locking would work by tilting
297 the SUN domains away from the ONM, it would be an elegant and simple solution to
298 prevent KASH binding. Our apo-structure now provides a framework for specifically
299 studying a self-locked state *in vivo*.
300 In summary, we report near-atomic resolution structures of several SUN2-KASH
301 complexes that shed light on the details of the mode of interaction. Also, we formally show
302 that a Sun trimer can engage with different KASH proteins simultaneously. Much is still to
303 be learned about the nuclear and cytoplasmic anchorage of LINC complexes, as well as
304 functional assembly states, important elements on the path toward a full molecular
305 understanding of mechanotransduction across the NE.

306
307

1
2
3
4
5
6
7
8
9
10
11
12
13
14
15
16
17
18
19
20
21
22
23
24
25
26
27
28
29
30
31
32
33
34
35
36
37
38
39
40
41
42
43
44
45
46
47
48
49
50
51
52
53
54
55
56
57
58
59
60
61
62
63
64
65

308 **Materials and Methods**

309

310 **Plasmid construction, protein expression and purification**

311 DNA sequences containing human SUN2 were cloned into a modified bicistronic ampicillin
312 resistant pETDuet-1 vector (EMD Millipore), superfolder GFP-KASH fusions (sfGFP) were
313 cloned and expressed into a modified ampicillin resistant vector, pET-30b(+) (EMD
314 Biosciences). Each KASH peptide (KASH1-6) was C-terminally fused to 6xHistidine-
315 sfGFP using inverse PCR. For crystallography, 6xHistidine tagged SUN2₅₂₂₋₇₁₇ was cloned
316 into the first multiple cloning site (MCS) and MBP-fused KASH4₃₇₉₋₄₀₄ was cloned into the
317 second MCS. For SUN2-KASH3₉₄₇₋₉₇₅ and SUN2-KASH5₅₄₂₋₅₆₂ the KASH peptides were
318 C-terminally fused to 6xHistidine-GB1 tags and SUN2₅₂₂₋₇₁₇ remained untagged. All SUN2
319 and KASH constructs were N-terminally fused with a human rhinovirus 3C protease
320 cleavage site.

321 Transformed LOBSTR(DE3)-RIL bacterial expression cells[34] were grown at 37 °C to an
322 OD₆₀₀ of 0.6, then shifted to 18 °C and induced with 0.2 M isopropyl β-D-1-
323 thiogalactopyranoside for 16 hours. Cells were harvested by centrifugation at 6000 g,
324 resuspended in lysis buffer (50 mM potassium phosphate, pH 8.0, 400 mM NaCl, 40 mM
325 imidazole) and lysed using an LM20 Microfluidizer Processor (Microfluidics). The lysate
326 was cleared by centrifugation at 10000 g for 25 minutes. The soluble fraction was
327 incubated with Nickel Sepharose 6 Fast Flow beads (GE Healthcare) for 30 minutes at 4
328 °C in batch. After the beads were washed with lysis buffer, the protein was eluted (10 mM
329 Tris/HCl pH 8.0, 150 mM NaCl, 250 mM imidazole). The protein was further purified by
330 size exclusion chromatography using an S75 or S200 16/60 column (GE Healthcare)
331 equilibrated in running buffer (10 mM Tris/HCl, pH 8.0, 150 mM NaCl, and 0.2 mM EDTA).

1
2
3
4
5
6
7
8
9
10
11
12
13
14
15
16
17
18
19
20
21
22
23
24
25
26
27
28
29
30
31
32
33
34
35
36
37
38
39
40
41
42
43
44
45
46
47
48
49
50
51
52
53
54
55
56
57
58
59
60
61
62
63
64
65

332 Protein affinity- and solubility-tags were removed with 3C protease and the protein
333 complexes were separated from fusion tags by a second size exclusion step using an S75
334 16/60 column, under the same conditions.

335

336 **Crystallization**

337 Purified Apo-SUN2₅₀₀₋₇₁₇ was concentrated to 7 mg/ml and crystallized in 14.5% (w/v)
338 polyethylene glycol (PEG) 3350, 100 mM potassium formate pH 8.0, and 200 mM sodium
339 bromide. Rhombohedral crystals appeared after 5 days at 18°C. SUN2-KASH3 complex
340 was concentrated to 5 mg/ml, and crystallized in 16-18% PEG3350, 100 mM ammonium
341 citrate pH 7.0, 100 mM BisTris/HCl pH 6.5, and 10 mM nickel (II) chloride. Large, plate-
342 shaped crystals grew within 2 days at 18°C. SUN2-KASH4 crystallized at 7 mg/ml in 17%
343 PEG3350, 200 mM magnesium chloride, and 100 mM BisTris/HCl pH 6.5. Crystals
344 appeared after 1 day and finished growing within 3 days, at 18°C. SUN2-KASH5 was
345 crystallized at 10 mg/ml, in 14% PEG3000, and 100 mM BisTris/HCl pH 6.5. Crystals
346 appeared and finished growing within 1-12 hours at 4°C. Crystals were cryoprotected in
347 their reservoir solution supplemented with 15% glycerol and flash-frozen in liquid nitrogen.
348 Diffraction data were collected at beamline 24ID-C at Argonne National Laboratories.

349

350 **X-ray data collection and structure determination**

351 All data processing was done using programs provided by SBgrid[35]. Data reduction was
352 carried out with HKL2000[36], molecular replacement with PHASER from the phenix
353 suite[37], using apo-SUN2 structure (PDB code 4DXT) that lacked the KASH lid as a
354 search model. The structures were manually built using Coot[38] and refined with
355 phenix.refine. Data collection and refinement statistics are summarized in Table 1.
356 Structure figures were created using PyMOL[39].

1
2
3
4
5
6
7
8
9
10
11
12
13
14
15
16
17
18
19
20
21
22
23
24
25
26
27
28
29
30
31
32
33
34
35
36
37
38
39
40
41
42
43
44
45
46
47
48
49
50
51
52
53
54
55
56
57
58
59
60
61
62
63
64
65

357

358 **Accession numbers**

359 Coordinates and structure factors have been deposited in the Protein Data Bank under
360 accession codes PDB **6WME** (SUN2-KASH3), **6WMD** (SUN2-KASH4), **6WMF** (SUN2-
361 KASH5), and **6WVG** (apo-SUN2).

362

363

1
2
3
4
5
6
7
8
9
10
11
12
13
14
15
16
17
18
19
20
21
22
23
24
25
26
27
28
29
30
31
32
33
34
35
36
37
38
39
40
41
42
43
44
45
46
47
48
49
50
51
52
53
54
55
56
57
58
59
60
61
62
63
64
65

364 **Acknowledgments**

365 This work was supported by NIH grant R01-AR065484 to T.U.S., the NIH Pre-Doctoral
366 Training Grant T32GM007287 (V.E.C.) and is based on research conducted at the
367 Northeastern Collaborative Access Team beamlines, which are supported by NIH grants
368 P30GM124165 and S10OD021527, and DOE contract DE-AC02-06CH11357. We thank
369 the staff at the Advanced Photon Source beamline 24-ID-C, K. Rajashankar in particular,
370 for assistance in data collection and space group analysis.

371

372 **References**

373 [1] K. Knockenhauer, T. Schwartz, The Nuclear Pore Complex as a Flexible and Dynamic
374 Gate, *Cell*. 164 (2016) 1162–1171. doi:10.1016/j.cell.2016.01.034.

375 [2] S.R. Wentz, M.P. Rout, The nuclear pore complex and nuclear transport., *Csh*
376 *Perspect Biol*. 2 (2010) a000562. doi:10.1101/cshperspect.a000562.

377 [3] D. Görlich, U. Kutay, Transport between the cell nucleus and the cytoplasm, *Annu Rev*
378 *Cell Dev Bi*. 15 (1999) 607 660. doi:10.1146/annurev.cellbio.15.1.607.

379 [4] G.G. Luxton, D.A. Starr, KASHing up with the nucleus: novel functional roles of KASH
380 proteins at the cytoplasmic surface of the nucleus, *Curr Opin Cell Biol*. 28 (2014) 69 75.
381 doi:10.1016/j.ceb.2014.03.002.

382 [5] D.A. Starr, H.N. Fridolfsson, Interactions between nuclei and the cytoskeleton are
383 mediated by SUN-KASH nuclear-envelope bridges., *Annu Rev Cell Dev Bi*. 26 (2010) 421
384 444. doi:10.1146/annurev-cellbio-100109-104037.

1
2
3
4
5
6
7
8
9
10
11
12
13
14
15
16
17
18
19
20
21
22
23
24
25
26
27
28
29
30
31
32
33
34
35
36
37
38
39
40
41
42
43
44
45
46
47
48
49
50
51
52
53
54
55
56
57
58
59
60
61
62
63
64
65

385 [6] Y.L. Lee, B. Burke, LINC complexes and nuclear positioning., *Semin Cell Dev Biol.* 82
386 (2018) 67–76. doi:10.1016/j.semcdb.2017.11.008.

387 [7] H. Hao, D.A. Starr, SUN/KASH interactions facilitate force transmission across the
388 nuclear envelope, *Nucleus.* 10 (2019) 73–80. doi:10.1080/19491034.2019.1595313.

389 [8] Accessorizing and anchoring the LINC complex for multifunctionality., *J Cell Biology.*
390 208 (2015) 11–22. doi:10.1083/jcb.201409047.

391 [9] D.A. Baum, B. Baum, An inside-out origin for the eukaryotic cell., *Bmc Biol.* 12 (2014)
392 76. doi:10.1186/s12915-014-0076-2.

393 [10] B.J. Mans, V. Anantharaman, L. Aravind, E.V. Koonin, Comparative genomics,
394 evolution and origins of the nuclear envelope and nuclear pore complex., *Cell Cycle*
395 (Georgetown, Tex). 3 (2004) 1612–1637.

396 [11] R. de Leeuw, Y. Gruenbaum, O. Medalia, Nuclear Lamins: Thin Filaments with Major
397 Functions, *Trends Cell Biol.* 28 (2018) 34–45. doi:10.1016/j.tcb.2017.08.004.

398 [12] B.A. Sosa, U. Kutay, T.U. Schwartz, Structural insights into LINC complexes., *Curr*
399 *Opin Struc Biol.* 23 (2013) 285–291. doi:10.1016/j.sbi.2013.03.005.

400 [13] A. Rothballer, U. Kutay, The diverse functional LINC complexes of the nuclear envelope to the
401 cytoskeleton and chromatin., *Chromosoma.* 122 (2013) 415–429. doi:10.1007/s00412-
402 013-0417-x.

403 [14] M. Crisp, Q. Liu, K. Roux, J.B. Rattner, C. Shanahan, B. Burke, P.D. Stahl, D. Hodzic,
404 Coupling of the nucleus and cytoplasm: role of the LINC complex., *J Cell Biology.* 172
405 (2006) 41–53. doi:10.1083/jcb.200509124.

1
2
3
4
5
6
7
8
9
10
11
12
13
14
15
16
17
18
19
20
21
22
23
24
25
26
27
28
29
30
31
32
33
34
35
36
37
38
39
40
41
42
43
44
45
46
47
48
49
50
51
52
53
54
55
56
57
58
59
60
61
62
63
64
65

406 [15] B.A. Sosa, A. Rothbaler, U. Kutay, T.U. Schwartz, LINC Complexes Form by Binding
407 of Three KASH Peptides to Domain Interfaces of Trimeric SUN Proteins., *Cell*. 149 (2012)
408 1035 1047. doi:10.1016/j.cell.2012.03.046.

409 [16] V.C. Padmakumar, T. Libotte, W. Lu, H. Zaim, S. Abraham, A.A. Noegel, J.
410 Gotzmann, R. Foisner, I. Karakesisoglou, The inner nuclear membrane protein Sun1
411 mediates the anchorage of Nesprin-2 to the nuclear envelope., *J Cell Sci*. 118 (2005) 3419
412 3430. doi:10.1242/jcs.02471.

413 [17] M.D. McGee, R. Rillo, A.S. Anderson, D.A. Starr, UNC-83 Is a KASH Protein Required
414 for Nuclear Migration and Is Recruited to the Outer Nuclear Membrane by a Physical
415 Interaction with the SUN Protein UNC-84, *Mol Biol Cell*. 17 (2006) 1790–1801.
416 doi:10.1091/mbc.e05-09-0894.

417 [18] J.A. Mellad, D.T. Warren, C.M. Shanahan, Nesprins LINC the nucleus and
418 cytoskeleton., *Curr Opin Cell Biol*. 23 (2011) 47 54. doi:10.1016/j.ceb.2010.11.006.

419 [19] A. Morimoto, H. Shibuya, X. Zhu, J. Kim, K.-I. Ishiguro, M. Han, Y. Watanabe, A
420 conserved KASH domain protein associates with telomeres, SUN1, and dynactin during
421 mammalian meiosis., *J Cell Biology*. 198 (2012) 165 172. doi:10.1083/jcb.201204085.

422 [20] R.E. Lindeman, F. Pelegri, Localized products of futile cycle/lrmp promote
423 centrosome-nucleus attachment in the zebrafish zygote., *Curr Biol*. 22 (2012) 843 851.
424 doi:10.1016/j.cub.2012.03.058.

425 [21] B. Burke, C.L. Stewart, Functional architecture of the cell's nucleus in development,
426 aging, and disease., *Curr Top Dev Biol*. 109 (2014) 1–52. doi:10.1016/b978-0-12-397920-
427 9.00006-8.

1
2
3
4
5
6
7
8
9
10
11
12
13
14
15
16
17
18
19
20
21
22
23
24
25
26
27
28
29
30
31
32
33
34
35
36
37
38
39
40
41
42
43
44
45
46
47
48
49
50
51
52
53
54
55
56
57
58
59
60
61
62
63
64
65

428 [22] C. Zhou, L. Rao, C.M. Shanahan, Q. Zhang, Nesprin-1/2: roles in nuclear envelope
429 organisation, myogenesis and muscle disease., *Biochem Soc T.* 46 (2018) 311 320.
430 doi:10.1042/bst20170149.

431 [23] H.F. Horn, Z. Brownstein, D.R. Lenz, S. Shivatzki, A.A. Dror, O. Dagan-Rosenfeld,
432 L.M. Friedman, K.J. Roux, S. Kozlov, K.-T. Jeang, M. Frydman, B. Burke, C.L. Stewart,
433 K.B. Avraham, The LINC complex is essential for hearing., *J Clin Invest.* 123 (2013) 740
434 750. doi:10.1172/jci66911.

435 [24] W. Wang, Z. Shi, S. Jiao, C. Chen, H. Wang, G. Liu, Q. Wang, Y. Zhao, M.I. Greene,
436 Z. Zhou, Structural insights into SUN-KASH complexes across the nuclear envelope, *Cell*
437 *Res.* 22 (2012) 1 13. doi:10.1038/cr.2012.126.

438 [25] N.E. Cain, Z. Jahed, A. Schoenhofen, V.A. Valdez, B. Elkin, H. Hao, N.J. Harris, L.A.
439 Herrera, B.M. Woolums, M.R.K. Mofrad, G.W.G. Luxton, D.A. Starr, Conserved SUN-
440 KASH Interfaces Mediate LINC Complex-Dependent Nuclear Movement and Positioning,
441 *Curr Biol.* 28 (2018) 3086-3097.e4. doi:10.1016/j.cub.2018.08.001.

442 [26] W.-J. Bao, Y.-G. Gao, Y.-G. Chang, T.-Y. Zhang, X.-J. Lin, X.-Z. Yan, H.-Y. Hu, Highly
443 efficient expression and purification system of small-size protein domains in *Escherichia*
444 *coli* for biochemical characterization, *Protein Express Purif.* 47 (2006) 599–606.
445 doi:10.1016/j.pep.2005.11.021.

446 [27] F.E. Demircioglu, T.U. Schwartz, Purification and Structural Analysis of SUN and
447 KASH Domain Proteins., *Methods Enzymol.* 569 (2016) 63 78.
448 doi:10.1016/bs.mie.2015.08.011.

1
2
3
4
5
6
7
8
9
10
11
12
13
14
15
16
17
18
19
20
21
22
23
24
25
26
27
28
29
30
31
32
33
34
35
36
37
38
39
40
41
42
43
44
45
46
47
48
49
50
51
52
53
54
55
56
57
58
59
60
61
62
63
64
65

449 [28] B. Ciani, S. Bjelic, S. Honnappa, H. Jawhari, R. Jaussi, A. Payapilly, T. Jowitt, M.O.
450 Steinmetz, R.A. Kammerer, Molecular basis of coiled-coil oligomerization-state
451 specificity., *P Natl Acad Sci Usa*. 107 (2010) 19850–5. doi:10.1073/pnas.1008502107.

452 [29] J.R. Partridge, T.U. Schwartz, Crystallographic and biochemical analysis of the Ran-
453 binding zinc finger domain., *J Mol Biol*. 391 (2009) 375–389.
454 doi:10.1016/j.jmb.2009.06.011.

455 [30] B.A. Sosa, A. Rothbaler, U. Kutay, T.U. Schwartz, LINC Complexes Form by Binding
456 of Three KASH Peptides to Domain Interfaces of Trimeric SUN Proteins, *Cell*. 149 (2012)
457 1035–1047. doi:10.1016/j.cell.2012.03.046.

458 [31] W. Chang, H.J. Worman, G.G. Gundersen, Accessorizing and anchoring the LINC
459 complex for multifunctionality., *J Cell Biology*. 208 (2015) 11–22.
460 doi:10.1083/jcb.201409047.

461 [32] G.W.G. Luxton, E.R. Gomes, E.S. Folker, E. Vintinner, G.G. Gundersen, Linear arrays
462 of nuclear envelope proteins harness retrograde actin flow for nuclear movement.,
463 *Science*. 329 (2010) 956–959. doi:10.1126/science.1189072.

464 [33] S. Nie, H. Ke, F. Gao, J. Ren, M. Wang, L. Huo, W. Gong, W. Feng, Coiled-Coil
465 Domains of SUN Proteins as Intrinsic Dynamic Regulators., *Structure*. 24 (2016) 80–91.
466 doi:10.1016/j.str.2015.10.024.

467 [34] K.R. Andersen, N.C. Leksa, T.U. Schwartz, Optimized *E. coli* expression strain
468 LOBSTR eliminates common contaminants from His-tag purification, *Proteins Struct Funct*
469 *Bioinform*. 81 (2013) 1857–1861. doi:10.1002/prot.24364.

1
2
3
4
5
6
7
8
9
10
11
12
13
14
15
16
17
18
19
20
21
22
23
24
25
26
27
28
29
30
31
32
33
34
35
36
37
38
39
40
41
42
43
44
45
46
47
48
49
50
51
52
53
54
55
56
57
58
59
60
61
62
63
64
65

470 [35] A. Morin, A. Morin, B. Eisenbraun, B. Eisenbraun, J. Key, J. Key, P.C. Sanschagrin,
471 P.C. Sanschagrin, M.A. Timony, M.A. Timony, M. Ottaviano, M. Ottaviano, P. Sliz, P. Sliz,
472 Collaboration gets the most out of software, *Elife*. 2 (2013) e01456 e01456.
473 doi:10.7554/elife.01456.

474 [36] Z. Otwinowski, W. Minor, Processing of X-ray diffraction data collected in oscillation
475 mode, *Methods in Enzymology*. 276 (1997) 307 326.

476 [37] D. Liebschner, P.V. Afonine, M.L. Baker, G. Bunkóczi, V.B. Chen, T.I. Croll, B. Hintze,
477 L.W. Hung, S. Jain, A.J. McCoy, N.W. Moriarty, R.D. Oeffner, B.K. Poon, M.G. Prisant,
478 R.J. Read, J.S. Richardson, D.C. Richardson, M.D. Sammito, O.V. Sobolev, D.H.
479 Stockwell, T.C. Terwilliger, A.G. Urzhumtsev, L.L. Videau, C.J. Williams, P.D. Adams,
480 Macromolecular structure determination using X-rays, neutrons and electrons: recent
481 developments in Phenix., *Acta Crystallogr Sect D Struct Biology*. 75 (2019) 861–877.
482 doi:10.1107/s2059798319011471.

483 [38] P. Emsley, B. Lohkamp, W.G. Scott, K. Cowtan, Features and development of Coot.,
484 *Acta Crystallogr Sect D Biological Crystallogr*. 66 (2010) 486 501.
485 doi:10.1107/s0907444910007493.

486 [39] D. WL, PyMOL, (2002).

487

488 **Figure legends**

489

490 **Fig. 1. Purification of SUN2-KASH complexes.**

491 **(A)** Purification scheme as employed for all SUN2-KASH complex preparations in this
492 study.

1
2
3
4
5
6
7
8
9
10
11
12
13
14
15
16
17
18
19
20
21
22
23
24
25
26
27
28
29
30
31
32
33
34
35
36
37
38
39
40
41
42
43
44
45
46
47
48
49
50
51
52
53
54
55
56
57
58
59
60
61
62
63
64
65

493 (B) SDS-PAGE analysis of purification steps of SUN2-KASH preparations. S, soluble
494 protein fraction from bacterial lysate. E, Ni-NTA affinity elution fraction. P, pure protein
495 complex after final gel filtration.

496

497 Fig. 2. **Comparison of Sun-KASH binding modes.**

498 (A) Space-filling cartoon representation of the two main binding modes, illustrated using
499 the best resolved complex structures for each class (left, SUN2-KASH1, PDB code 4DXR;
500 right, SUN2-KASH4. 6WMD). SUN2 trimer subunits in shades of blue. KASH1 peptide in
501 white, KASH4 peptide in orange. Note the kinked vs. straight conformation of the KASH-
502 peptide.

503 (B) Superposition of the five SUN2-bound KASH peptides, including important SUN2
504 binding elements. The SUN2 conformation is very similar in all five complex structures.

505

506 Fig. 3. **Details of SUN2-bound KASH peptides.**

507 (A) KASH1-5 are illustrated in stick representation and oriented identically as they are
508 positioned in the SUN2 binding interface. The two views provide detail over the entire
509 KASH sequence. Important positions are numbered, starting at position '0', the very C-
510 terminal residue. Notice position -11, which is where the 90° kink in KASH1 and KASH2
511 occurs.

512 (B) Structure-based sequence alignment of the 5 KASH peptides for which complex
513 structures with SUN2 exist. Sequence conservation indicated in a blue color gradient.

514 Lower case letters represent residues in the crystallized construct that were invisible, i.e.
515 presumably disordered, in the respective crystal structures.

516

517 Fig. 4. **Details of the SUN2 cation loop.**

1
2
3
4
5
6
7
8
9
10
11
12
13
14
15
16
17
18
19
20
21
22
23
24
25
26
27
28
29
30
31
32
33
34
35
36
37
38
39
40
41
42
43
44
45
46
47
48
49
50
51
52
53
54
55
56
57
58
59
60
61
62
63
64
65

518 (A) Overview of a SUN2 monomer, with key structural elements labeled. Purple sphere
519 represents the potassium ion that is bound in most SUN2 structures.

520 (B) Detailed view of the canonical potassium coordination in the cation loop, illustrated
521 using the SUN2-KASH3 coordinates. $2F_o-F_c$ electron density map contoured at 1.5σ .

522 (C) The SUN2-KASH4 complex constitutes an exception, as it shows two water molecules
523 positioned in the area that is typically occupied by a potassium ion. $2F_o-F_c$ electron density
524 map contoured at 1.5σ .

525

526 **Fig. 5. Details of the “PPPX” binding vicinity.**

527 (A) Detailed view of the SUN2 area in close contact with the C-terminal 3 residues of the
528 KASH peptide. In the KASH1/2 bound structures the cysteine 601/705 pair is best
529 modeled as oxidized, as shown. $2F_o-F_c$ electron density map contoured at 1.5σ .

530 (B) The same detailed view as in (A) but showing the KASH4 interaction. Here, the
531 cysteine 601/705 pair is best modeled as reduced. $2F_o-F_c$ electron density map contoured
532 at 1.5σ .

533

534 **Fig. 6. Head-to-head packed apo-SUN2 homotrimers may represent a self-locked**
535 **state.**

536 (A) Packing interface in the crystal between two adjacent apo-SUN2 homotrimers. The
537 KASH-lid (orange) is prominently involved in the 2380 \AA^2 interface.

538 (B) The same packing interface as in (A) but showing the SUN2-KASH4 interaction
539 instead. Notice how the two heterohexamers are much further apart and how the packing
540 interface is significantly smaller. (C) and (D) are close-ups of the head-to-head interfaces
541 shown in (A) and (B), respectively. Highly conserved residues involved in the postulated
542 self-locked, apo-SUN2 homo-hexamers are labeled. The labeled interaction network is

1
2
3
4
5
6
7
8
9
10
11
12
13
14
15
16
17
18
19
20
21
22
23
24
25
26
27
28
29
30
31
32
33
34
35
36
37
38
39
40
41
42
43
44
45
46
47
48
49
50
51
52
53
54
55
56
57
58
59
60
61
62
63
64
65

543 repeated 6 times in the apo-SUN2 hexameric interface. In the KASH-bound interface,
544 these residues have no comparable role.

545

546 **Fig. 7. A Sun trimer can bind different KASH peptides simultaneously.**

547 **(A)** SUN2₅₂₂₋₇₁₇ was recombinantly co-expressed in bacteria with two KASH peptides, one
548 His-tagged, the other GFP-tagged. The complexes were co-purified using Ni-NTA affinity,
549 establishing that a SUN2 trimer can simultaneously bind at least two different KASH
550 peptides. The SDS-PAGE shows three KASH combinations and a negative control
551 experiment. S, soluble bacterial protein extract; U, unbound fraction; E, elution fraction
552 from Ni-NTA affinity experiment.

553 **(B)** Representative gel filtration experiment using SUN2₅₂₂₋₇₁₇ / 6xHis-GB1-KASH2/ GFP-
554 KASH1 complex purified via Ni-NTA affinity. Chromatogram shows that GFP-KASH1
555 coelutes with the main protein peak. SDS-PAGE analysis (inset) of gel filtration fractions
556 (range indicated in red) confirms that all three input proteins coelute, indicating stable
557 complex formation.

558

559 **Fig. S1. Details of SUN2-bound KASH peptides, including the SUN2 surface.**

560 **(A)** KASH peptides lined up in the same way as in Fig. 3 but including the SUN2 surface.

561

562

563

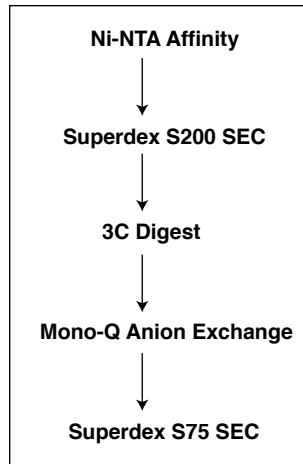
Table 1

PDB Code	hsSUN2-KASH3 6WME	hsSUN2-KASH4 6WMD	hsSUN2-KASH5 6WMF	hsSUN2 6WMG
Data Collection				
Space group	P6 ₃ 22	P6 ₃ 22	H32	H32
Cell dimensions				
<i>a</i> , <i>b</i> , <i>c</i> (Å)	78.7, 78.7, 173.3	80.8, 80.8, 173.9	78.4, 78.4, 249.4	79.2, 79.2, 199.5
Resolution (Å)	53.57-1.53 (1.59-1.53)	69.94-1.50 (1.53-1.50)	83.15-2.60 (2.69-2.60)	56.51-1.90 (1.95-1.90)
R _{p.i.m.} (%)	1.4 (68.0)	2.1 (51.4)	2.5 (46.6)	4.2 (59.9)
I/σ(I)	68.3 (1.0)	55.6 (2.0)	37.3 (0.9)	24.0 (1.4)
CC _{1/2} (%)	99.9 (60.8)	99.9 (61.8)	99.9 (50.9)	99.6 (65.2)
Completeness (%)	98.6 (87.1)	99.9 (98.6)	99.2 (94.1)	99.0 (97.0)
Redundancy	32.8 (25.4)	23.3 (19.9)	15.9 (6.3)	3.7 (3.4)
Refinement				
Resolution (Å)	53.57-1.53 (1.59-1.53)	69.94-1.50 (1.53-1.50)	83.15-2.60 (2.73-2.60)	56.51-1.90 (1.95- 1.90)
No. reflections	47678	54661	9383	19072
R _{work} /R _{free}	20.7/23.8	16.3/18.5	22.1/28.7	17.1/22.1
No. atoms	1980	2106	1694	1672
Protein	1736	1739	1681	1541
Solvent, ions	244	367	13	131
B factors (Å ²)	40.4	30.3	96.4	52.3
Protein	38.9	28.3	96.6	52.2
Solvent, ions	50.7	40.1	77.9	53.9
Root mean squared deviations				
Bond lengths (Å)	0.006	0.008	0.008	0.017
Bond angles (°)	0.948	0.980	1.035	1.454

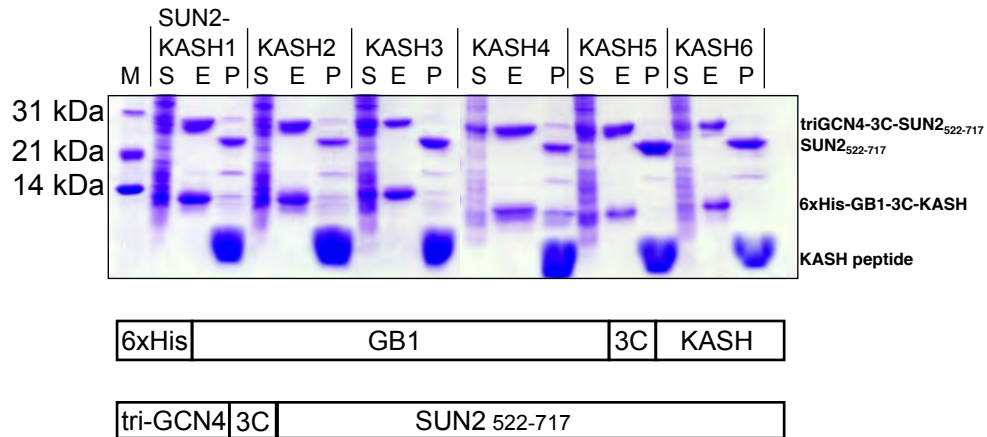
Fig. 1

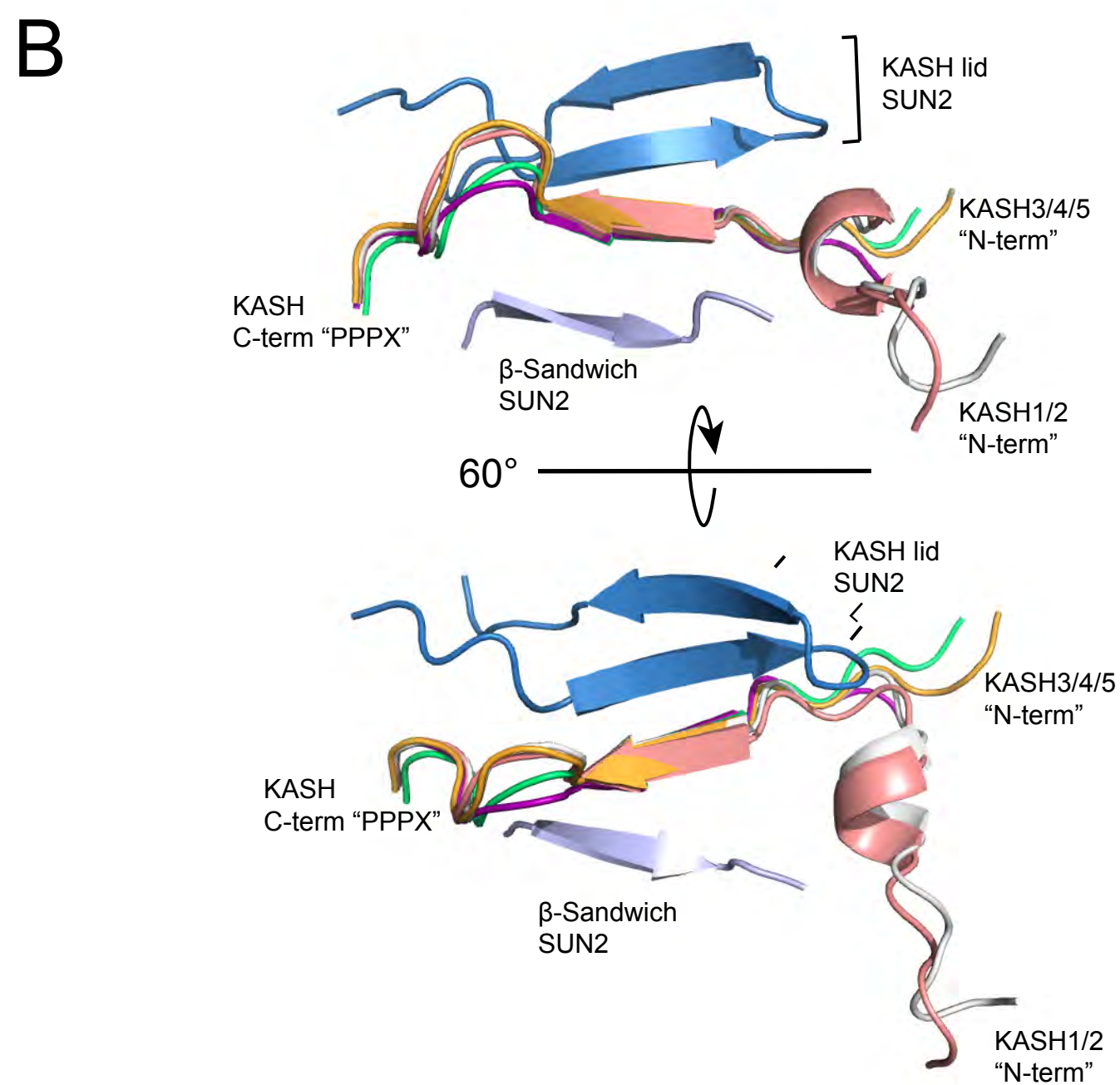
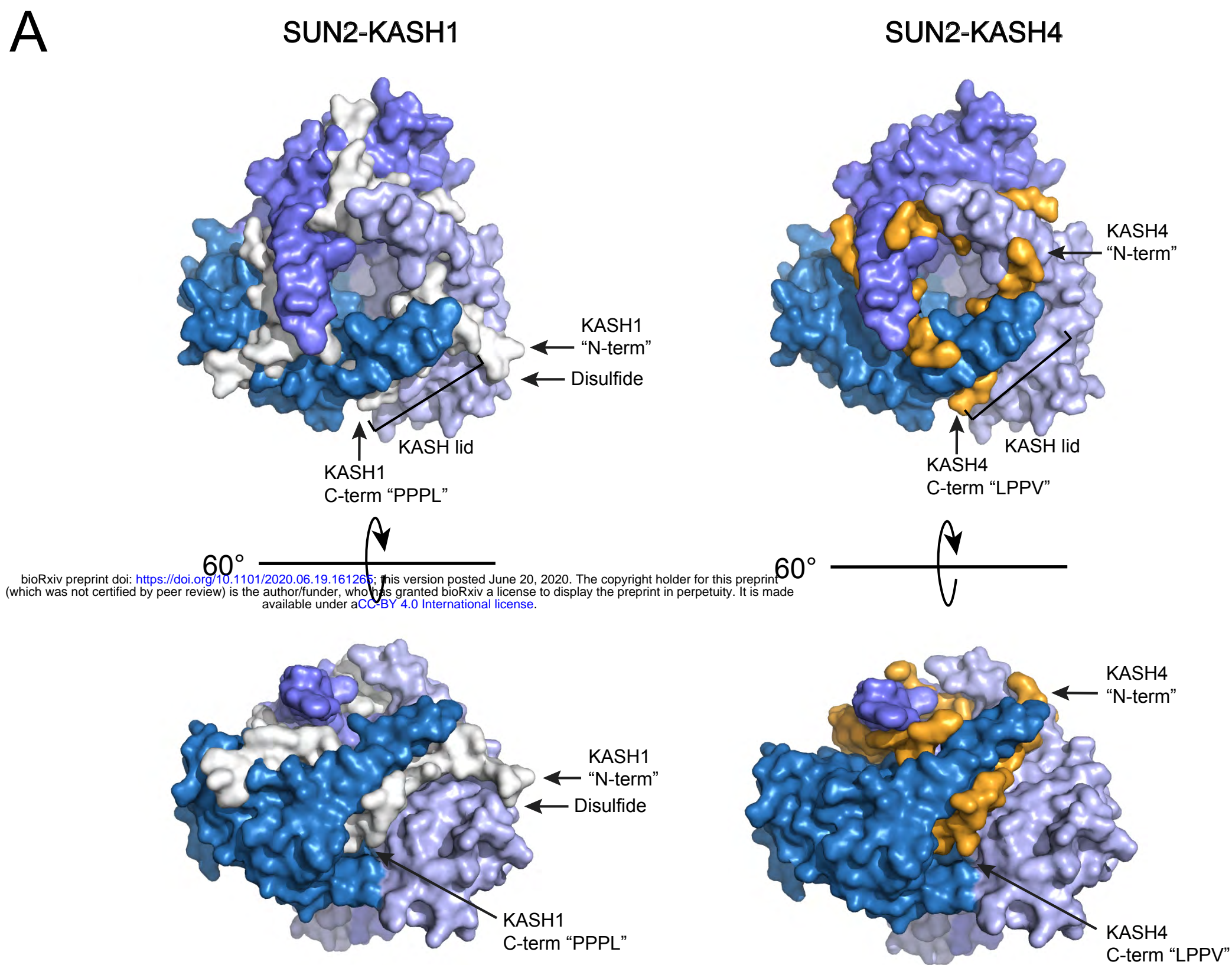
A

Purification Scheme

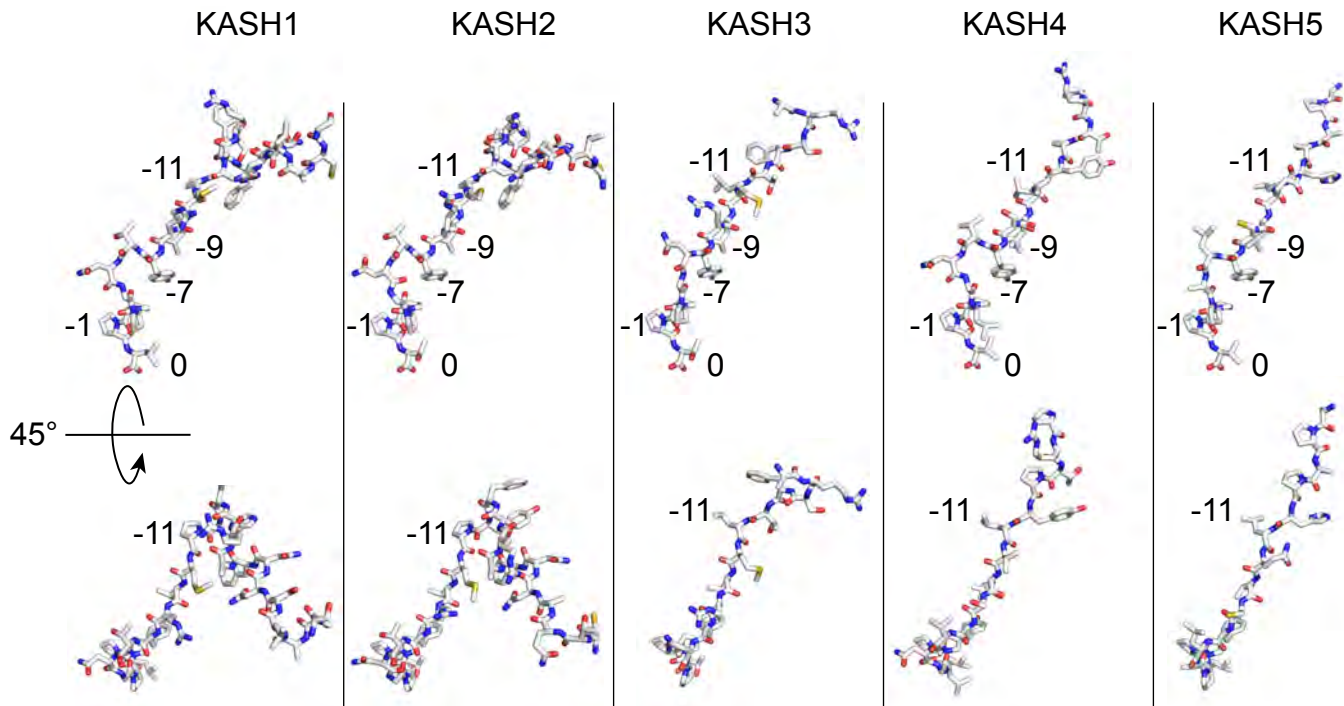


B





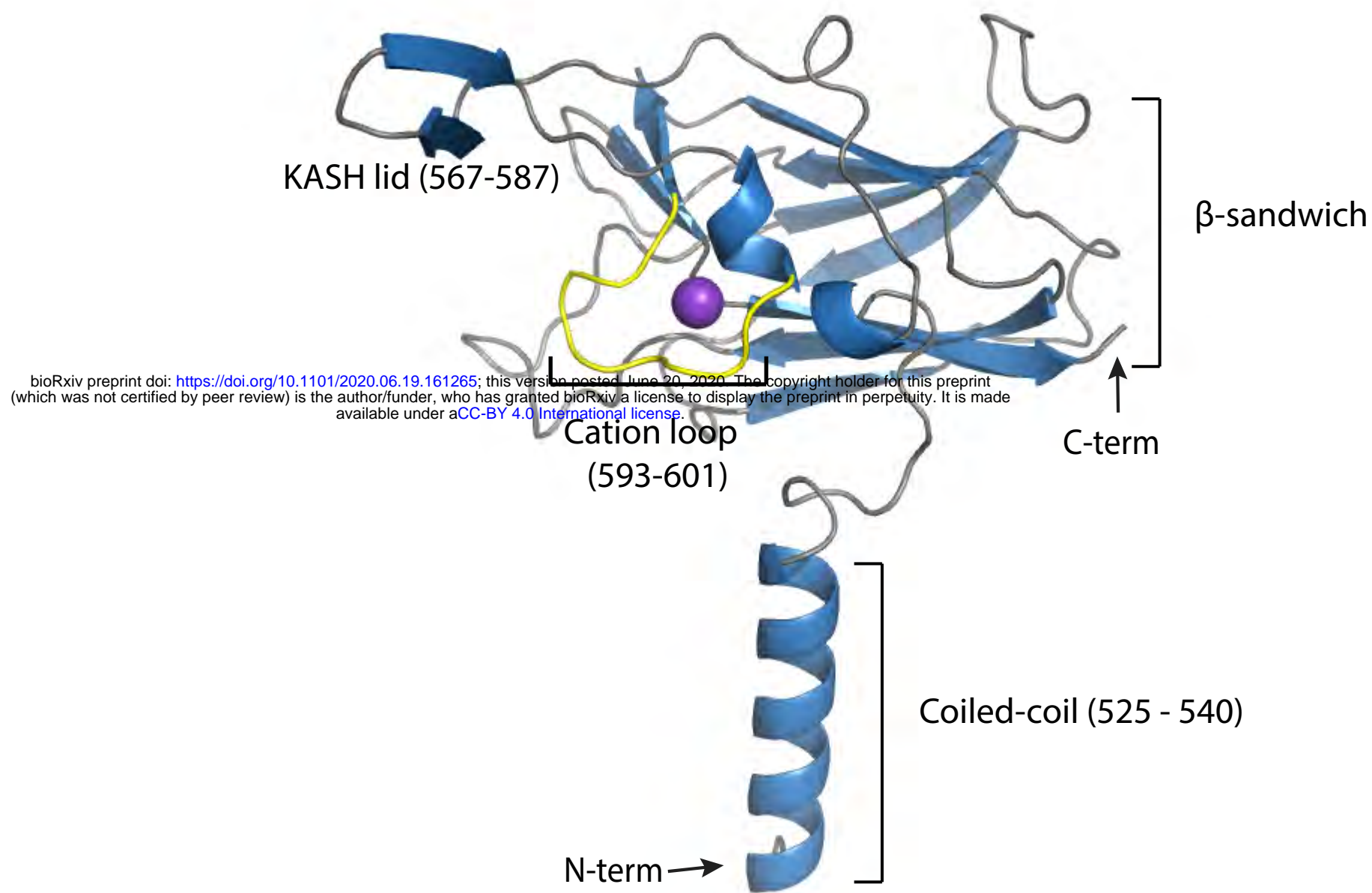
A



B

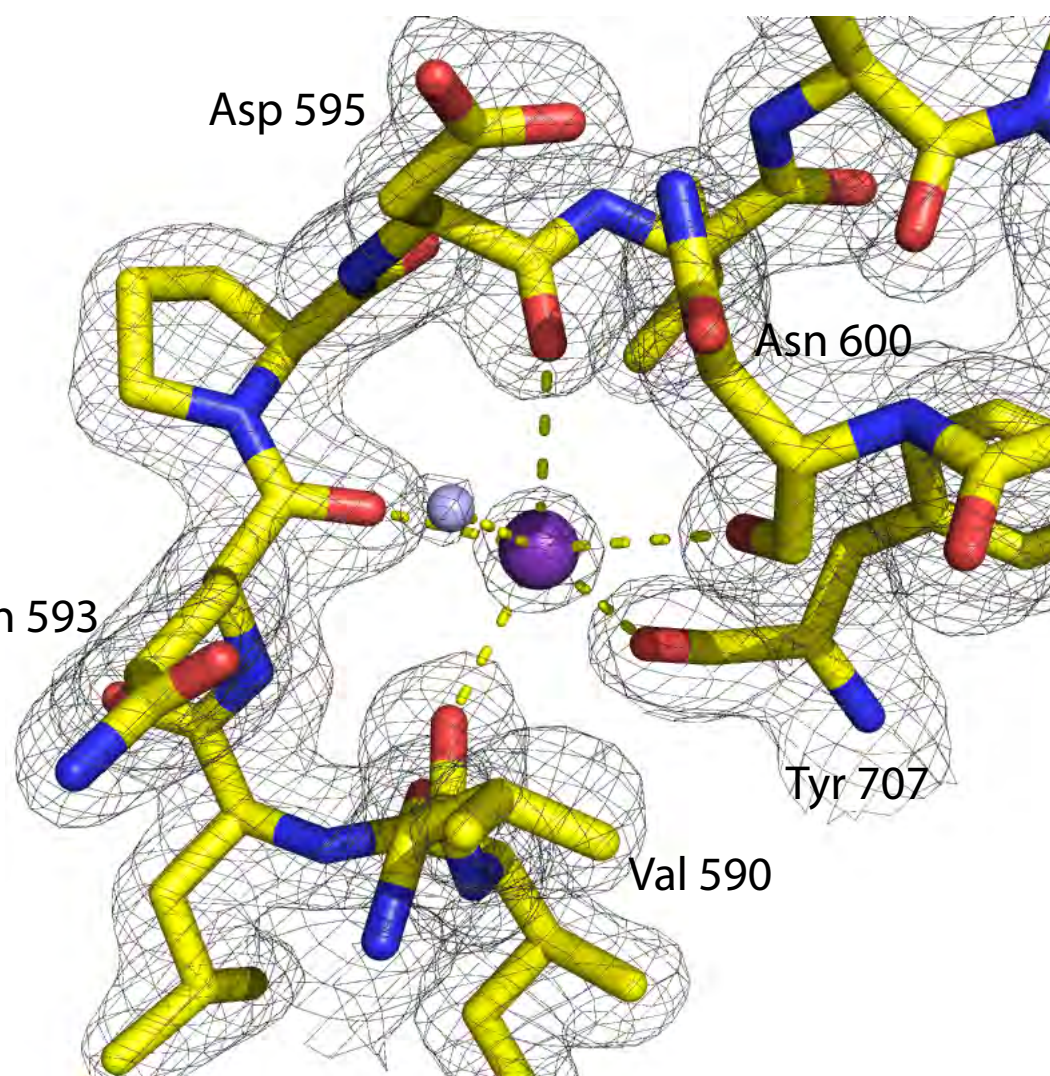
				-23		-11	-9	-7		0																			
<i>H. sapiens</i>	KASH1	8769	<i>s e e d y</i>	S	C	A	L	S	N	N	F	A	R	S	F	H	P	M	L	R	Y	T	N	G	P	P	P	L	8797
<i>H. sapiens</i>	KASH2	6857	<i>- e e d y</i>	S	C	T	Q	A	N	N	F	A	R	S	F	Y	P	M	L	R	Y	T	N	G	P	P	P	T	6885
<i>H. sapiens</i>	KASH3	948	<i>- e e d r</i>	<i>s c t l a n n</i>	F	A	R	S	F	T	L	M	L	R	Y	N	-	G	P	P	P	T	975						
<i>H. sapiens</i>	KASH4	377	<i>- - s g g p c c s h a r i</i>	P	R	T	P	Y	L	V	L	S	Y	V	N	G	L	P	P	V	404								
<i>H. sapiens</i>	KASH5	542	<i>- - - - -</i>	<i>g p s p p p</i>	T	W	P	H	L	Q	L	C	Y	L	-	Q	P	P	P	V	562								

A



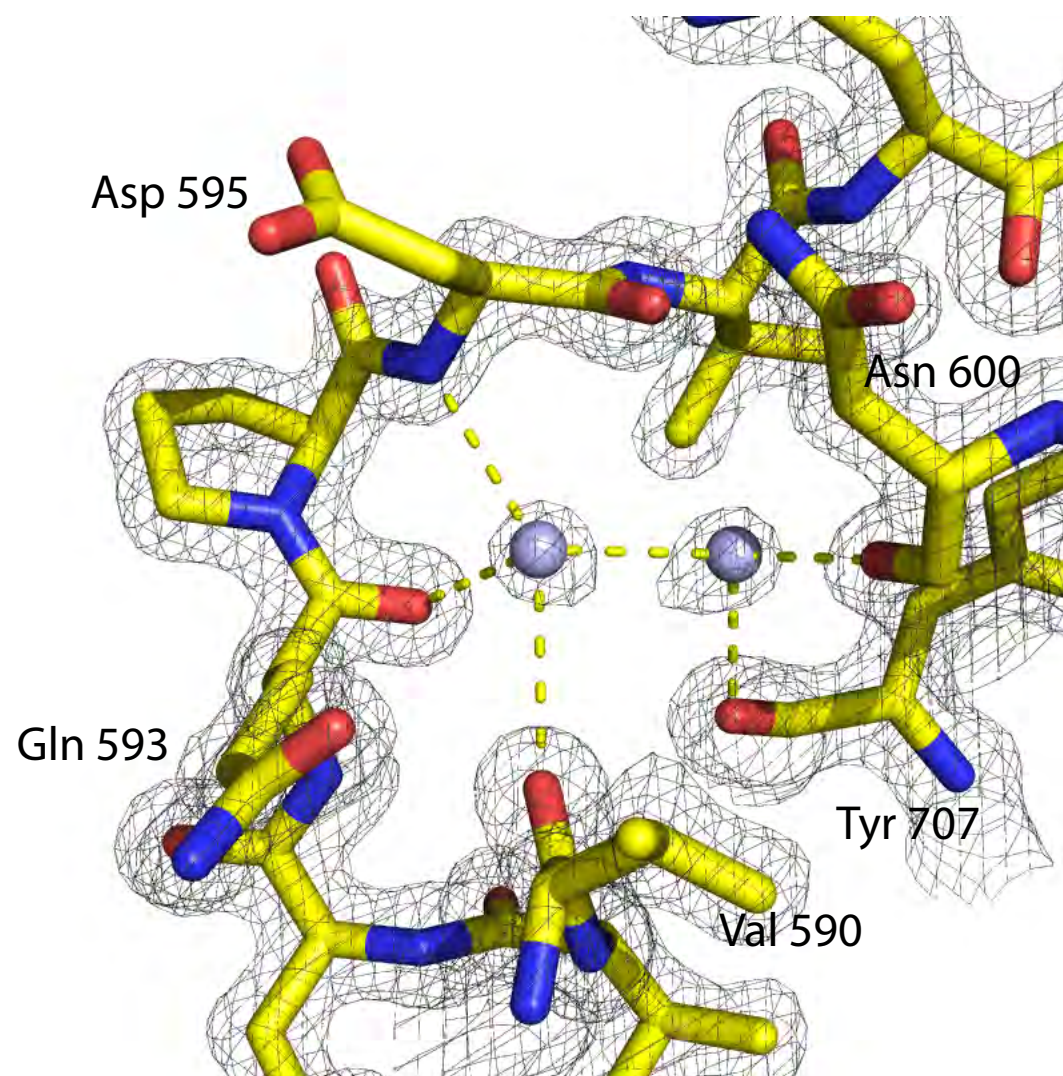
B

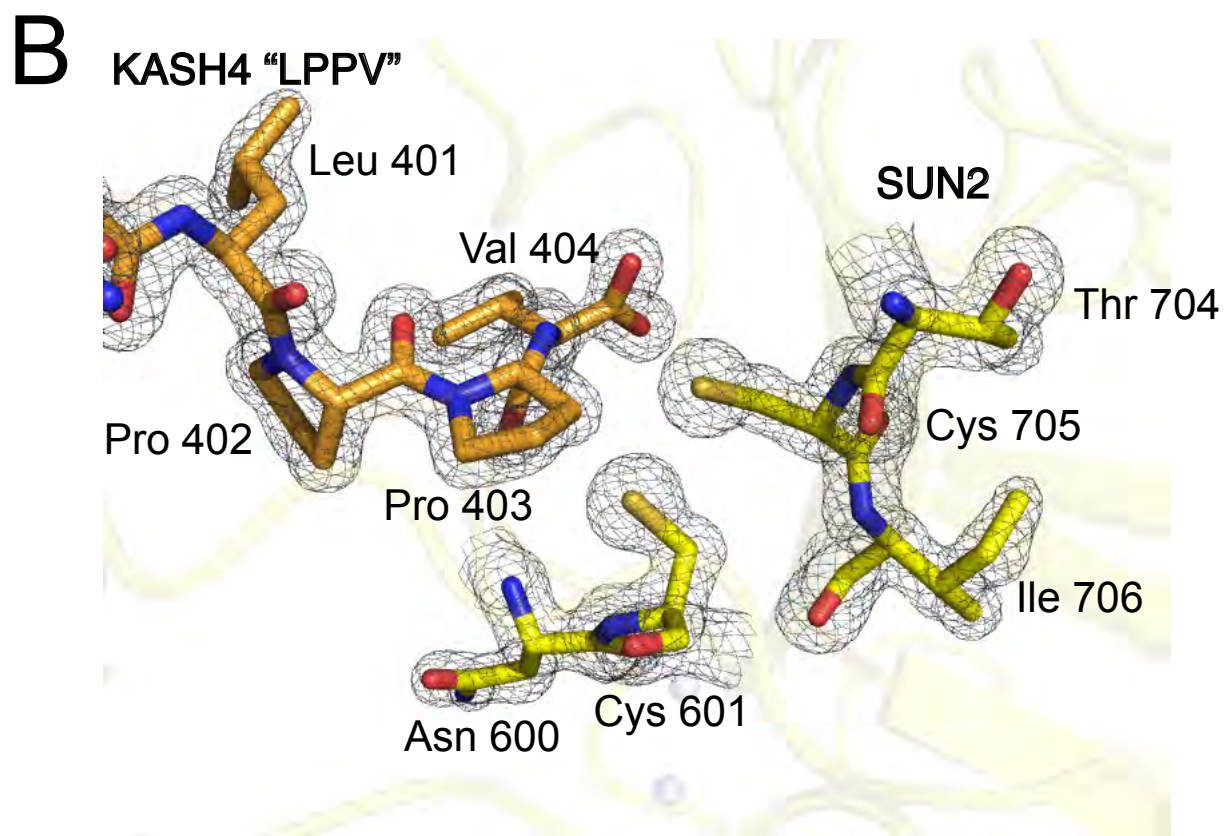
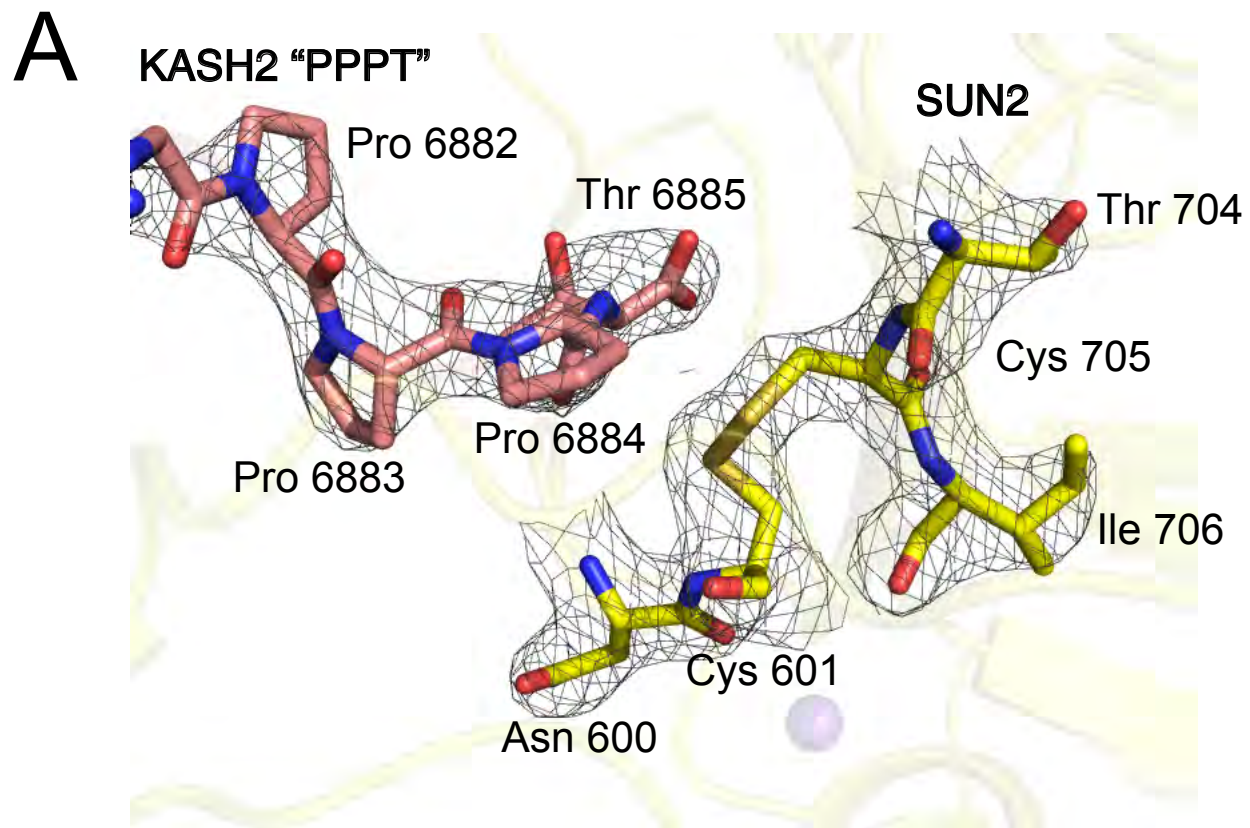
SUN2-KASH3



C

SUN2-KASH4





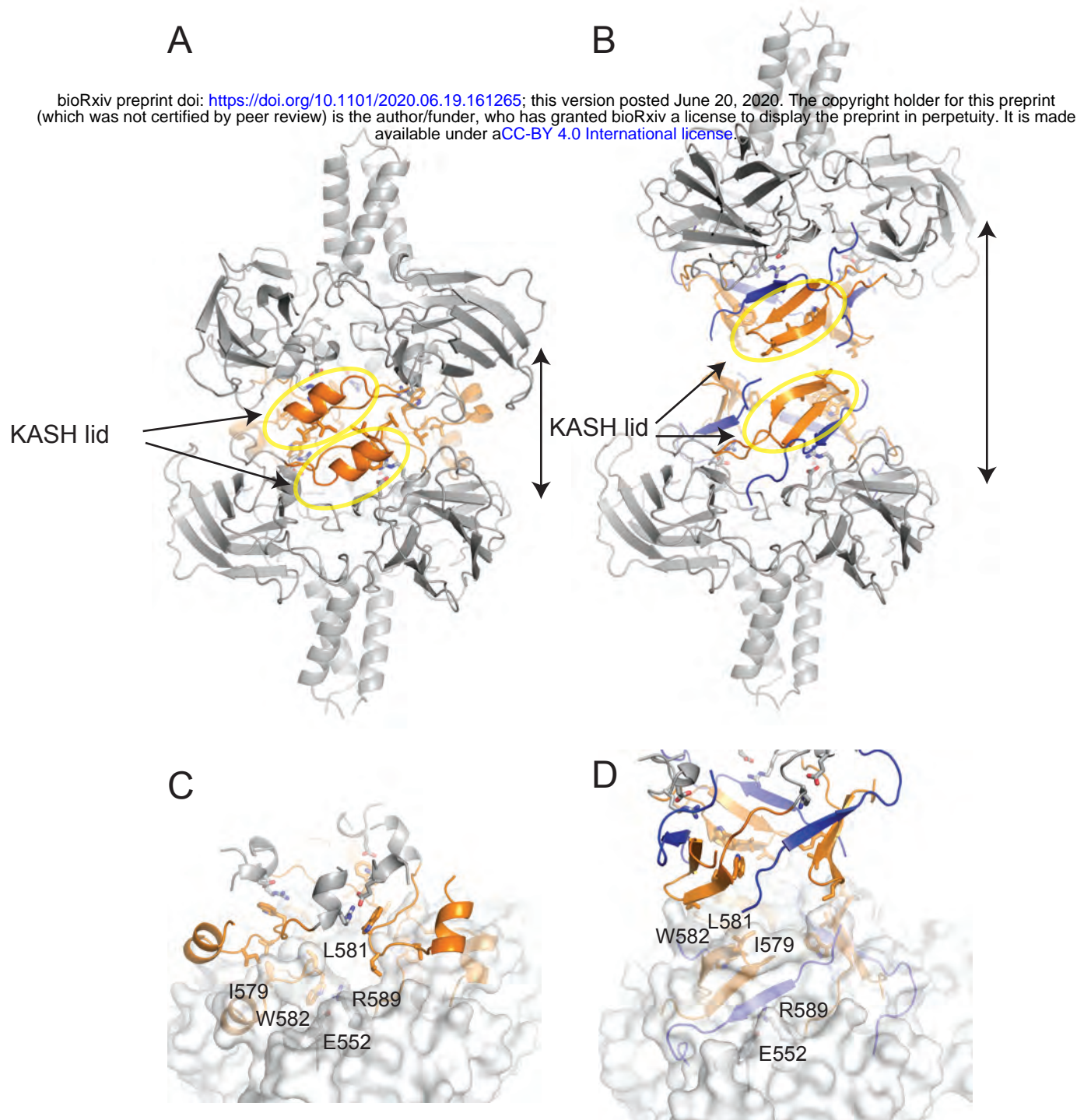
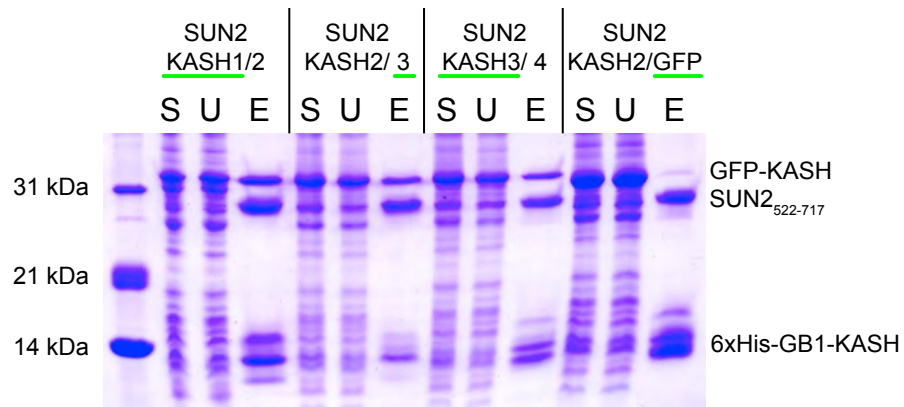


Fig. 7

A



B

